Proceedings of ICRC 2001: 1751 © Copernicus Gesellschaft 2001

ICRC 2001

Ulysses High Energy Telescope Measurements of the Isotopic Composition of Galactic Cosmic Rays for the Elements Be to Ni

J. J. Connell

The Laboratory for Astrophysics and Space Research, The Enrico Fermi Institute, The University of Chicago, 933 E. 56th Street, Chicago IL 60637, USA

Abstract. We report new and revised high resolution measurements of the isotopic composition of Galactic cosmic rays in the Solar system using data from the High Energy Telescope (HET) on the *Ulysses* Spacecraft. These data have significantly improved statistics compared with our earlier measurements. Mass resolution varies from ~0.08 to ~0.31 u at observed energies of ~100 to ~300 MeV/u for elements Be to Ni.

1. Introduction

The isotopic composition of Galactic cosmic rays provides unique information on crucial questions concerning the astrophysics of cosmic rays. Corrected for propagation, cosmic ray isotopic abundance measurements provide clues to the source of the cosmic rays and insight into Galactic chemical evolution. Secondary radioisotopes test models of cosmic ray propagation and confinement in the Galaxy, including the extent of a possible Galactic magnetic halo. Secondary electron capture nuclides address cosmic ray reacceleration.

The *Ulysses* Mission is a joint NASA and ESA project. The spacecraft was launched on Oct. 6, 1990 on the shuttle *Discovery* and, via a gravitation assist at Jupiter, was inserted into a Solar orbit with a perihelion of 1.34 AU, aphelion of 5.4 AU and an ~80^{o} heliographic inclination. The data presented here covers the period from launch through the middle of 2000, corresponding to double the statistics in some of our previous papers. This is also our first report on the isotopes of B, Ar, K, Ca, Cr and Co.

The measurements presented here are of isotopic abundances in the Solar system. A full interpretation awaits completion our ongoing analysis of elemental composition. The measurements here are nonetheless presented in the expectation that they will be of use to others modeling cosmic rays. Prior reports have been made on the isotopic composition of C to Si (Connell, and Simpson, 1997a), S (Thayer, 1997), Mn (DuVernois, 1997), Fe and Ni (Connell, and Simpson, 1997b) with source abundance estimates; on the isotopic abundances of Be (Connell, 1998), Al (Simpson and Connell, 1998) and Cl (Connell, DuVernois and Simpson, 1998) and Mn (DuVernois, 1997; Wuosmaa et al. 1998) as radioactive chronometers of propagation; and of V as a potential test of cosmic ray reacceleration (Connell and Simpson, 1999).

Correspondence to: connell@odysseus.uchicago.edu

2. Data Analysis

The HET has two sets of three single-dimensional position-sensing Si detectors (PSD's) of 1100 μm thickness. Below the PSD's are six 5000 μm Si detectors (K's) that provide mass and charge determination by the multiple $\Delta E/\Delta x$ versus residual energy method for events stopping in the second through sixth K detectors. A Si detector (A) and scintillator shield (S) identify events that exit the detector stack (Simpson et al. 1992).

The analysis began by requiring the projected trajectory of each heavy ion into the detector after the stopping detector have a radius of less than 20 mm. This meant that a nucleus, if it had continued beyond the apparent stopping detector, would have encountered an active region of the next detector rather than dead material. An approximate charge determination was made using the "ZCAL" method (Lau, 1985) where the range of an ion is approximated by a power law in energy per nucleon so,

$$R = \kappa_0 \frac{A}{Z^2}\left(\frac{E}{A}\right)^{\alpha} \quad (1)$$

where α and κ_0 are constants. From the energy losses in the stopping detector (E_0) and the detector above it (E_{-1}), and under the approximation $A = 2Z$,

$$R_0 = \frac{\kappa}{Z^{\alpha+1}} E_0^{\alpha} \quad (2)$$

$$R_0 + T_{-1}\sec(\theta) = \frac{\kappa}{Z^{\alpha+1}}\left(E_0 + E_{-1}\right)^{\alpha} \quad (3)$$

where R_0 is the (unknown) range in the stopping detector, T_{-1} is the thickness of the detector above, and θ is the angle of incidence determined from the PSD's. α and κ are empirically determined using, in this case, Fe events. By solving both equations, the charge is determined.

For events of each charge stopping in K2 to K6, four ratios of energy depositions in the D's were made: $E_2/(E_1 + E_3)$, $E_3/(E_2 + E_4)$, $E_4/(E_3 + E_5)$ and $E_5/(E_4 + E_6)$. A maximum likelihood fit was made to the resulting distributions for each element and a cut of 2.5 σ applied.

The PSD's are oriented at rotational intervals of 60° to provide redundancy in case of a failure during flight. This also results in a self-calibrating system. Using five PSD (say D1, and D3 to D6), the trajectory of a particle was determined; this provided a prediction of the position in the sixth detector (D2 in the example) which was compared to the measured position. By a process of iteration, non-linear corrections for the PSD's were determined.

The mass of events was found using an extension of the ZCAL method with equation (1) used to determine A. In this case, α and κ were treated as slowly varying functions of energy and charge. Fits were made for ^{12}C, ^{16}O, ^{28}Si and ^{56}Fe to obtain α and κ tables. Other elements were analyzed using the table having the nearest Z. This process was applied not only for the stopping K and the K above it, but also for each K. A weighted mean was taken as the best estimate of the mass.

The HET has experienced temperatures from ~25° to -15° C. Fits to the Fe data show a temperature coefficient of ~103 ppm/°C. This is less than the intrinsic temperature response of Si detectors (~ -160 ppm/°C) and reflects a small positive temperature coefficient in the in-flight calibrator. The data also exhibits a temporal drift of ~0.189 ppt/year. These corrections were applied to the isotope data.

With multiple mass determinations, a 2.0 σ consistency cut was applied to obtain the final data set. No radius cut was made (or needed) on the final selected data. A quiet time selection is made to avoid contamination by Solar energetic particles. Figure 1 shows the results for Fe.

Gaussian peaks were fit to the mass histogram for each element using the maximum likelihood method. The peak position for the most abundance isotope was free, but the other peak positions were determined by fitting a single center-to-center spacing parameter. A single fractional σ was fit. A flat background was also fit. The area of the Gaussian for each isotope was thus determined.

The resulting abundance ratios were corrected to the average energy of each element in the data by integrating over the predicted spectral shape for each isotope's energy interval in the instrument, also taking into account the change in geometry factor with depth in the instrument. To cover the wide range of solar conditions since the launch of *Ulysses*, modulation parameters (Φ) for each year (except 1991, which also includes days 296 to 365 of 1990) were found, mainly based on carbon data from IMP-8 and *Pioneer*-10. The average Solar radius of the *Ulysses* spacecraft for each period was included. A modulation boundary of 100 AU was assumed.

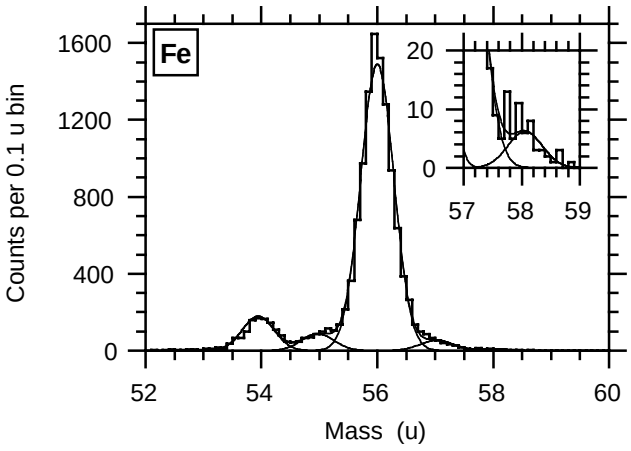

Fig. 1. *Ulysses* HET Mass histogram of Fe isotopes with maximum likelihood fit. Figure shows 12860 event with a mass resolution of σ = 0.285 ± 0.003 u.

Table 1 shows the results. The number of events, mean energy and mass resolution are shown for each element, together with the corrected isotopic abundance ratios. Errors are statistical only. The background (over one mass unit) are show relative to the most abundance isotope.

3. Conclusions

The measurements presented here are generally in good agreement with earlier HET measurements but with much enhanced statistics. The additional elements also expand the data-base of isotopic abundance measurements. It should be emphasized that the analysis used here was chosen to obtain reliable isotopic abundances and may well introduce significant element to element biases. These results thus cannot be used for elemental abundances.

The interpretation of these results awaits the completion of the elemental analysis, an ongoing project. These are required to constrain the cosmic ray propagation model and to determine source elemental abundances in conjunction with the isotopic abundances.

Acknowledgments: The HET was designed by J. A. Simpson and R. Jacquet and constructed by the staff of the Laboratory for Astrophysics and Space Research. A. J. Tuzzolino and E. LaRue made essential contributions to the design and development of the position sensing Si detectors. The University of Chicago. Special thanks are due to C. Lopate for Solar modulation parameters. This research was supported in part by NASA/JPL Contract 955432.

Table 1

Element	Number of Events	Average E (MeV/u)	Mass resolution σ (u)	Isotopic Ratio	Ratio (%)
Be	2214	106	0.075 ± 0.002	$^{9}Be/^{7}Be$	55.5 (+8.2, -7.5)
				$^{10}Be/^{7}Be$	11.7 (+1.5, -1.7)
				Bgnd/^{7}Be	0.80 (+0.18. -0.14)
B	10759	112	0.107 ± 0.001	$^{10}B/^{11}B$	42.0 (+0.9, -1.0)
				Bgnd/^{11}B	0.347 (+0.034, -0.032)
C	56328	128	0.1100 ± 0.0005	$^{13}C/^{12}C$	5.88 ± 0.13
				Bgnd/^{12}C	0.333 (+0.014, -0.0088)
N	14206	138	0.124 ± 0.001	$^{15}N/N$	50.7 (+1.2, -0.9)
				Bgnd/^{15}N	< 1.7
O	67532	152	0.1255 ± 0.005	$^{17}O/^{16}O$	0.960 (+0.043, -0.053)
				$^{18}O/^{16}O$	1.263 (+0.046, -0.067)
				Bgnd/^{16}O	0.392 (+0.013, -0.010)
Ne	10803	168	0.146 ± 0.001	$^{21}Ne/^{20}Ne$	22.39 (+0.80, -0.70)
				$^{22}Ne/^{20}Ne$	59.1 ±1.4
				Bgnd/^{20}Ne	0.419 (+0.045, -0.040)
Mg	16959	190	0.161 ± 0.001	$^{25}Mg/^{24}Mg$	20.85 (+0.54, -0.49)
				$^{26}Mg/^{24}Mg$	22.78 (+0.51, -0.60)
				Bgnd/^{24}Mg	0.457 (+0.032, -0.031)
Al	2649	199	0.177 +/ 0.003	$^{26}Al/^{27}Al$	5.89 (+0.53, -0.56)
				Bgnd/^{27}Al	0.094 (+0.036, -0.026)
Si	13722	209	0.179 ± 0.001	$^{29}Si/^{28}Si$	8.22 (+0.34, -0.28)
				$^{30}Si/^{28}Si$	6.31 ± 0.27
				Bgnd/^{28}Si	0.239 (+0.025, -0.021)
S	2383	224	0.226 ± 0.005	$^{33}S/^{32}S$	17.2 (+1.9, -0.9)
				$^{34}S/^{32}S$	22.8 (+1.9, -1.2)
				$^{36}S/^{32}S$	0.56 (+1.13, -0.05)
				Bgnd/^{32}S	< 0.91
Cl	463	232	0.25 ± 0.01	$^{35}Cl/Cl$	63.8 (+5.0, -5.5)
				$^{36}Cl/Cl$	5.4 (+2.3, -0.8)
				$^{37}Cl/Cl$	30.8 (+3.80, -3.0)
				Bgnd/^{35}Cl	< 1.3
Ar	951	240	0.240 ± 0.007	$^{36}Ar/Ar$	39.3 (+2.8, -2.4)
				$^{37}Ar/Ar$	20.1 ± 1.8
				$^{38}Ar/Ar$	35.0 ± 2.5
				$^{40}Ar/Ar$	5.56 (+0.53, -1.45)
				Bgnd/^{36}Ar	< 0.17
K	776	244	0.27 ± 0.01	$^{40}K/^{39}K$	64.2 ± 6.2
				$^{41}K/^{39}K$	46 ± 5
				Bgnd/^{39}K	0.5 ± 0.2
Ca	2006	246	0.266 ± 0.007	$^{41}Ca/^{40}Ca$	21 (+6, -2)
				$^{42}Ca/^{40}Ca$	50 (+5, -4)
				$^{43}Ca/^{40}Ca$	54 (+7, -4)
				$^{44}Ca/^{40}Ca$	55 (+11, -4)
				Bgnd/^{40}Ca	< 0.25

Table 1 (Continued)

Element	Number of Events	Average E (MeV/u)	Mass resolution σ (u)	Isotopic Ratio	Ratio (%)
Ti	1801	262	0.257 ± 0.006	^{44}Ti/Ti	0.82 (+0.19, -0.26)
				^{46}Ti/Ti	29.0 ± 1.6
				^{47}Ti/Ti	29.8 ± 1.7
				^{48}Ti/Ti	31.0 ±1.7
				^{49}Ti/Ti	7.9 (+0.8, -0.9)
				^{50}Ti/Ti	1.5 (+0.4, -0.3)
				Bgnd/^{48}Ti	< 2.0
V	876	267	0.256 ± 0.009	^{50}V/^{49}V	51.5 (+4.9, -4.7)
				^{51}V/^{49}V	42.3 (+4.2, -4.1)
				Bgnd/^{49}V	0.55 (+0.21, -0.17)
Cr	1827	276	0.256 ± 0.007	^{50}Cr/^{52}Cr	43.6 (+3.3, -2.8)
				^{51}Cr/^{52}Cr	54.7 (+3.7 -3.5)
				^{53}Cr/^{52}Cr	15.0 (+2.4, -1.3)
				^{54}Cr/^{52}Cr	8.2 (+1.8, -0.8)
				Bgnd/^{52}Cr	< 0.5
Mn	1098	285	0.262 ± 0.008	^{54}Mn/^{53}Mn	22.3 (+2.8, -2.5)
				^{55}Mn/^{53}Mn	74.0 ± 5.4
				Bgnd/^{53}Mn	0.73 (+0.22, -0.19)
Fe	12860	290	0.285 ± 0.003	^{54}Fe/^{56}Fe	11.20 (+0.26, -0.75)
				^{55}Fe/^{56}Fe	5.67 (+0.38, -0.22)
				^{57}Fe/56Fe	3.69 (+0.32, -0.18)
				^{58}Fe/^{56}Fe	(0.44 +0.20, -0.03)
				Bgnd/56Fe	< 0.69
Co	64	300	0.30 ± 0.03	^{57}Co/Co	41 ± 11
				^{59}Co/Co	59 ± 14
				Bgnd/^{59}Co	< 2.7
Ni	616	304	0.31 ± 0.01	^{59}Ni/^{58}Ni	2.1 (+1.5, -1.2)
				^{60}Ni/^{58}Ni	43.4 (+4.5, -4.2)
				^{61}Ni/^{58}Ni	4.1 ± 1.4
				^{62}Ni/^{58}Ni	5.3 ± 1.4
				^{64}Ni/^{58}Ni	0.6 (+0.8, -0.3)
				Bgnd/^{58}Ni	< 0.7

References

Connell, J. J. and Simpson, J. A., 1997a, "High Resolution Measurements of the Isotopic Composition of Galactic Cosmic Ray C, N, O, Ne, Mg and Si from the *Ulysses* HET," *Proc. 25th ICRC* (Durban, South Africa), **3**, 381.

Connell, J. J. and Simpson, J. A., 1997b, "Isotopic Abundances of Fe and Ni in Galactic Cosmic Ray Sources," *Ap. J. Lett.*, **475**, L61.

Connell, J. J. and Simpson, J. A., 1999, "*Ulysses* HET Measurements of Electron-capture Secondary Isotopes: Testing the Role of Cosmic Ray Reacceleration," *Proc. 26th ICRC* (Salt Lake City, USA) , **3**, 33-36.

Connell, J. J., DuVernois, M. A. and Simpson, J. A., 1998, "Galactic Cosmic Ray ^{36}Cl Clock: *Ulysses* HET Results," *Ap. J. Lett.*, **509**, L97.

Connell,, J. J., 1998, "Galactic Cosmic Ray Confinement Time: *Ulysses* HET Measurements of the Secondary Radio-Nuclide ^{10}Be," *Ap. J. Lett.*, **501**, L59.

DuVernois, M. A.: 1997, `Galactic Cosmic-Ray Manganese: *Ulysses* High Energy Telescope Results', *Ap. J*, **481**, 241.

Lau, Koon J., 1985, *A Cerenkov-de-Cerenkov Detector for High Energy Cosmic Ray Isotopes and an Accelerator Study of ^{40}Ar & ^{56}Fe Fragmentation*, CalTech Ph.D. thesis.

Simpson, J. A. et al., 1992, "The *Ulysses* Cosmic Ray and Solar Particle Investigation," *Astron. and Ap. Suppl.*, **92**, 365.

Simpson, J. A. and Connell, J. J., 1998, "Cosmic Ray ^{26}Al and Its Decay in the Galaxy," *Ap. J. Lett.*, **497**, L85**.**

Thayer, M. R.: 1997, "An Investigation Into Sulfur Isotopes in the Galactic Cosmic Rays," *Ap. J.*, **482**, 792

Wuosmaa, A. H.. et al. ,1998, "The β^+ Decay Partial Half Life of ^{54}Mn and Cosmic Ray Chronometry," *Phys. Rev. Let.***, 80**, 2085.